PL-TR--92-1075

AD-A270 101

PL-TR--
92-1075

CHARACTERIZATION OF VAPOR PLUME SPECIES AND DEPOSITION RESIDUES RESULTING FROM PULSED LASER ABLATION OF A GRAPHITE/ EPOXY COMPOSITE

Robert E. Roybal
Charles J. Miglionico
Dr Charles Stein
Larry E. Murr
Kenneth A. Lincoln

August 1993

Final Report

Approved for public release; distribution is unlimited.

PHILLIPS LABORATORY
Space and Missiles Technology Directorate
AIR FORCE MATERIEL COMMAND
KIRTLAND AIR FORCE BASE, NM 87117-5776

This final report was prepared by the Phillips Laboratory, Kirtland Air Force Base, New Mexico, under Job Order 2864TR07. The project officer-in-charge was Mr Robert Roybal (VTSI).

This technical report has been reviewed and is approved for publication.

ROBERT E. ROYBAL
Project Officer

FOR THE COMMANDER

DR CHARLES STEIN
Chief, Space Environmental Effects Branch

EUGENE R. DIONNE, Col, USAF
Director of Space and Missiles Technology

REPORT DOCUMENTATION PAGE

Form Approved
OMB No 0704-0188

1. AGENCY USE ONLY *(Leave blank)*

2. REPORT DATE
August 1993

3. REPORT TYPE AND DATES COVERED
Final Jun 92 - Jan 93

4. TITLE AND SUBTITLE
CHARACTERIZATION OF VAPOR PLUME SPECIES AND DEPOSITION RESIDUES RESULTING FROM PULSED LASER ABLATION OF A GRAPHITE/EPOXY COMPOSITE

5. FUNDING NUMBERS
PE: 62302F
PR: 2864
TA: TR
WU: 07

6. AUTHOR(S)
Robert E. Roybal, Charles J. Miglionico, Dr Charles Stein, Larry E. Murr*, and Kenneth A. Lincoln**

7. PERFORMING ORGANIZATION NAME(S) AND ADDRESS(ES)
Phillips Laboratory
3550 Aberdeen Avenue, SE
Kirtland AFB, NM 87117-5776

8. PERFORMING ORGANIZATION REPORT NUMBER
PL-TR--92-1075

9. SPONSORING/MONITORING AGENCY NAME(S) AND ADDRESS(ES)

10. SPONSORING/MONITORING AGENCY REPORT NUMBER

11. SUPPLEMENTARY NOTES
*L. Murr is with the University of Texas at El Paso, Department of Metallurgical and Materials Engineering, El Paso, TX 79968, and **K. Lincoln is with the Eloret Institute, NASA Ames Research Center, Moffett Field, CA 94035.

12a. DISTRIBUTION/AVAILABILITY STATEMENT
Approved for public release; distribution is unlimited.

12b. DISTRIBUTION CODE

13. ABSTRACT *(Maximum 200 words)*
A modified time-of-flight mass spectrometer (TOFMS) fitted with a special collection stage for carbon-coated transmission electron microscope specimen grids is used to monitor laser-pulse ablation products from graphite/epoxy composite targets. Scanning electron microscopy observations show ablation damage to consist of matrix pyrolysis, fiber fracture, and spallation of fragments which include elemental hydrogen, carbon epoxide, and acetylene groups. Transmission electron microscope examination of specimen grids showed a variety of crystals and polycrystalline hexagonal graphites having a wide range of shapes including spheres and faceted polyhedra and platelets, textured flake structures, and microrosettes. These observations lend some credibility to a model for laser-shock and pyrolysis effects which creates molecular plume fragments and deposition fragments of hexagonal graphite.

14. SUBJECT TERMS
Graphite/Epoxy Composite, Laser Ablation, Laser Shock, Time-of-Flight Mass Spectrometry (TOFMS), Vapor Blow-off, Transmission Electron Microscopy (TEM)

15. NUMBER OF PAGES
30

16. PRICE CODE

17. SECURITY CLASSIFICATION OF REPORT	18. SECURITY CLASSIFICATION OF THIS PAGE	19. SECURITY CLASSIFICATION OF ABSTRACT	20. LIMITATION OF ABSTRACT
Unclassified	Unclassified	Unclassified	SAR

ACKNOWLEDGEMENTS

This work was supported by the Phillips Laboratory of the USAF and by the NASA Ames Research Center and aided in particular by the work of Dr. K. A. Lincoln. We are also grateful to Drs. A. H. Advani and C. S. Niou for their help with some of the TEM sample analyses.

CONTENTS

FIGURES

1.0 INTRODUCTION

There has been considerable interest over the past several decades in the interactions of laser beams with a variety of materials, especially those involved in aerospace applications (Refs. 1 and 2). More recently these interactions have been of particular interest in the context of space defense systems such as the U. S. Strategic Defense Initiative system (or Star Wars concepts) and laser blow-off of spacecraft materials (Ref. 3), especially laser-composite interactions. These interactions can involve a variety of energy deposition phenomena which include laser shock effects (including shock pressure effects, spallation, and shock heating) (Ref. 4), and constrained plasma (pyrolysis) effects (Ref. 5) which can lead to a host of chemical effects, blow-off of discrete matter, and deposition of recombined components (including molecular fragments) as well as direct or redeposition of molecular fragments (Ref. 6). Earlier efforts to investigate some of the phenomena involving laser blow-off of spacecraft materials attempted to develop analytical methodologies to predict target materials' response to repetitive (pulsed) laser irradiation. These methodologies included the vapor plume characterization: velocity, expansion angle, and mass fraction. These more recent investigations, unlike those originally conceived to simply explore degradation of target materials in laser impact situations (Refs. 1 and 2), have been more concerned with the contamination of neighboring surfaces by deposition of interaction and reaction products. The specific concerns in these processes include the contamination or alteration of sensor, optical, or other protective surfaces by blow-off or plume debris.

In the research to be reported here, a time-of-flight mass spectrometer (TOFMS) analytical technique developed at the NASA Ames Research Center to dynamically sample vapor plumes was modified to collect deposition fractions (or fragments) of plumes from a pulsed-laser-irradiated graphite-epoxy (G/E) composite. This technique included a TOFMS equipped with a special collection system employing carbon support grids which would collect deposited plume material that could be examined in a transmission electron microscope (TEM). The hope was to examine the ablation site, the plume composition and any residual deposition fragments.

2.0 EXPERIMENTAL PROCEDURES

In this investigation, a TOFMS capable of producing time-resolved spectra along the duration of a vapor plume was incorporated into a pulsed-laser/materials interaction chamber. The laser wavelength was 1.06 μm with a pulse duration of 800 μs. The beam spot size was nominally 6 mm^2 corresponding to an energy density of 3 to 36 Ca/J/cm^2 or a peak irradiance of 5 to 60 Kw/cm^2. The TOFMS system itself utilized a nude electron source operating continuously at a preset repetition rate of 30 to 40 kHz. This system, illustrated schematically in Figure 1, is a modification of a system described previously by K. A. Lincoln (Ref. 3).

In addition to the TOFMS system integrated into the laser interaction regime to examine the blow-off or plume material, a vapor collection stage was incorporated to allow 3-mm electron microscope carbon-coated grids to be exposed to the vapor plume. Located a distance of 5.75 cm and an angle of 64° from the sample surface, the grid collector surfaces could be exposed to the vapor plume one at a time by rotating the collection stage by an aperture which shielded exposed or unexposed grid collector surfaces as shown in Figure 1.

The target materials, consisting of 1.2-cm squares of G/E composites containing 60 percent volume fraction of Hercules (1M6-G-12k) graphite fibers in an epoxy matrix (LRF 387 resin system containing Epon 828, NAM, and a TERCOL 1000 plasticizer, Ref. 3) were introduced into the test chamber in Figure 1 through a loading port and were positioned at a focal distance of 33 cm from the laser focusing lens to maintain a spot size of 6 mm^2. Samples were irradiated with single pulses and their "vapor pulse" spectra examined in the TOFMS.

The collection grids for TEM were examined following single and multiple-pulse experiments. These examinations involved both conventional and scanning transmission electron microscopy (CTEM and STEM) which included energy-dispersive X-ray spectrometry, selected-area electron diffraction and microdiffraction analysis, and lattice imaging of deposited, electron transparent fragments.

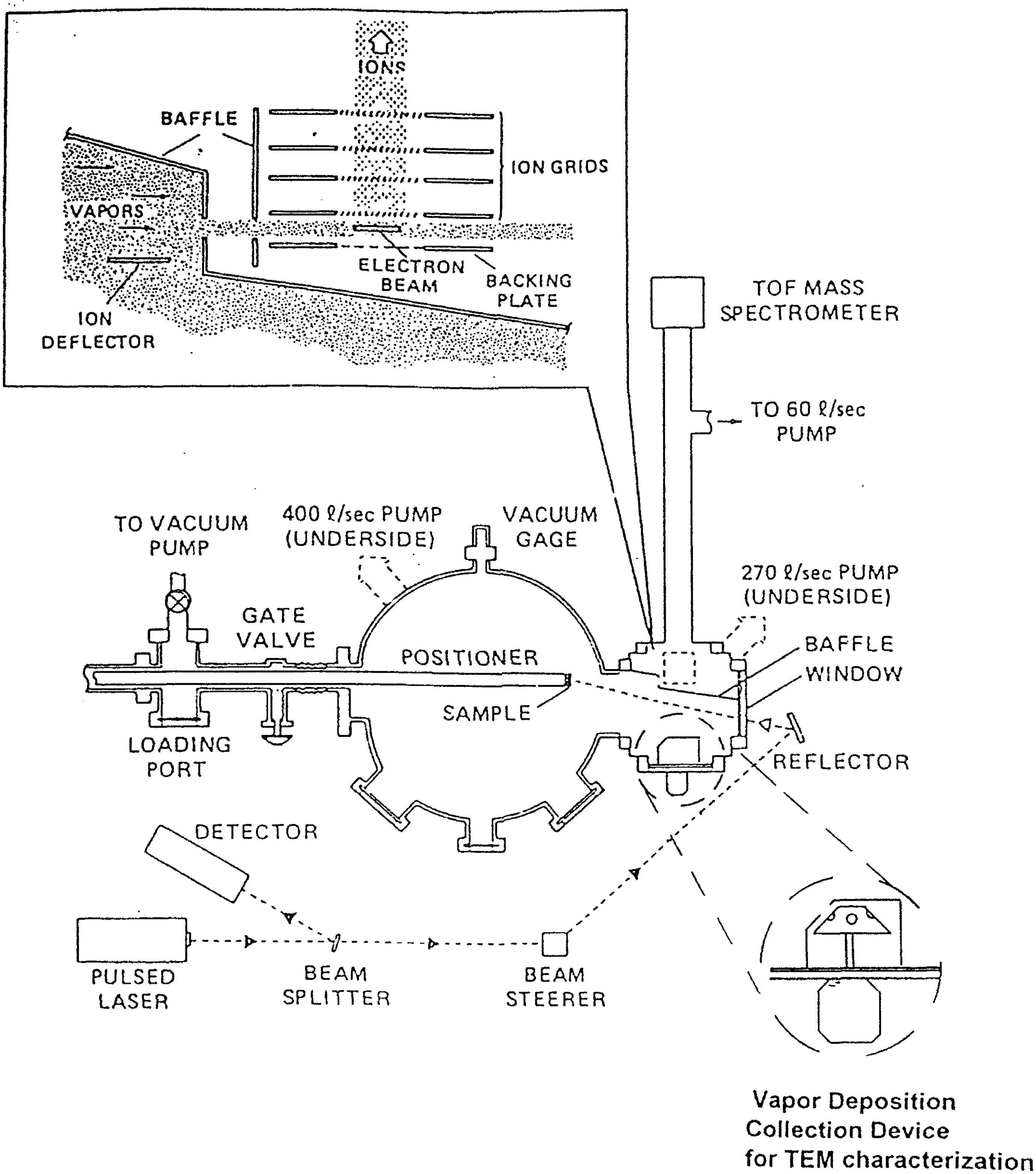

Figure 1. Schematic diagram of the advanced laser/TOFMS system with TEM grid specimen collection stage.

3.0 RESULTS AND DISCUSSION

Figure 2 presents a rather practical (and macroscopic) overview of the laser-G/E target materials interaction involving localized damage to the irradiated focal area on the specimen surface. These residual damage micro-structures show graphite fiber fracture and matrix ablation. Evidence of local melt or vapor redeposition is also illustrated.

Figure 3 shows a typical, multi-shot (laser pulse) spectrum for a vapor plume created in an ablation process as illustrated typically in Figure 2. There are several notable features (pyrolysis products) of this spectrum: free hydrogen, free carbon, epoxide fragments (free radicals), acetylenes (fixed gases) and impurities. Other notable fragments include CH, CH_2 and CH_3 groups. These constituents can be visualized with the aid of some generalized chemical structures for epoxy resins illustrated schematically in Figure 4. The epoxide group (C_2H_30) shown in Figure 4 contains a covalent half-bond available for bonding. For solid resins n, in Figure 4, is 2 or greater. The epoxy and hydroxyl groups (-OH) are the reaction sites for cross-linking.

The presence of contaminants such as Na, K, Fe, Ca, Cl, Al, and water vapor (H_20) occur primarily on or very near the specimen surface, and this is illustrated to some extent by comparing time-resolved, multi-pulse spectra as illustrated in Figure 5 which shows a reduction in water vapor from the first to fourth pulse, and little other contamination as a result of having simply wiped the target surface with a lint-free cloth. Figure 5 also shows a marked reduction in the epoxide component with repeated laser pulsing and an increase in C_n and the acetylene family fragments. The resulting ablation sequence after larger numbers of pulses generally showed spectra typical for graphitic materials (Ref. 7).

When looking at the vapor plume in a time-resolved fashion as in Figure 5, it was found that the species possessed different generation times and life spans. The expected order of species generation was epoxides, acetylene, and finally carbons. This was based on

(a) Broken, exposed graphite fibers in ablation zone.

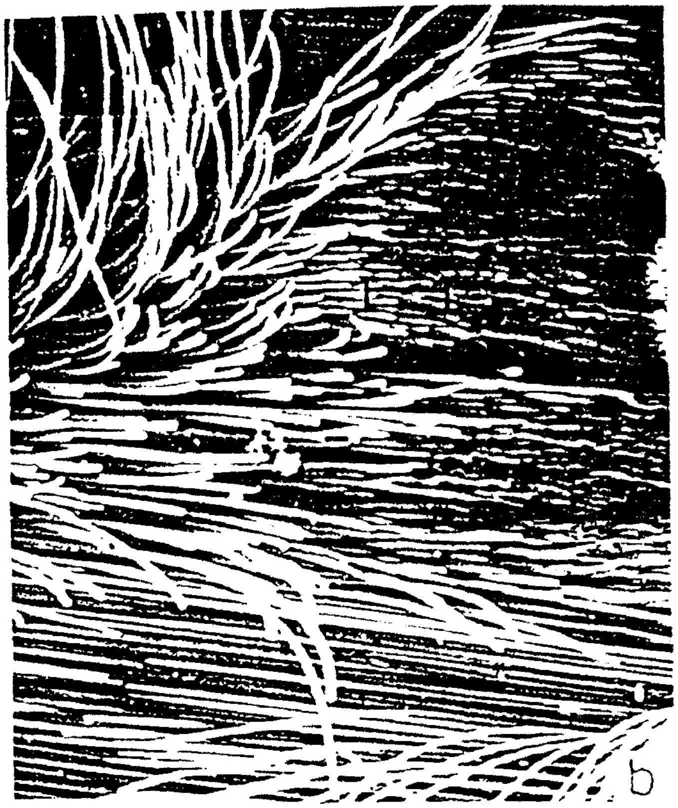

(b) Broken, exposed graphite fibers in ablation zone.

(c) Ablation tunnel showing fiber damage detail.

(d) Melt/deposition hemisphere growth in ablation zone.

Figure 2. Scanning electron microscope views of laser-ablated G/E specimen areas. Magnification markers correspond to 1 mm in (a), 0.1 mm in (b), 20 μm in (c), and 2 μm in (d), respectively.

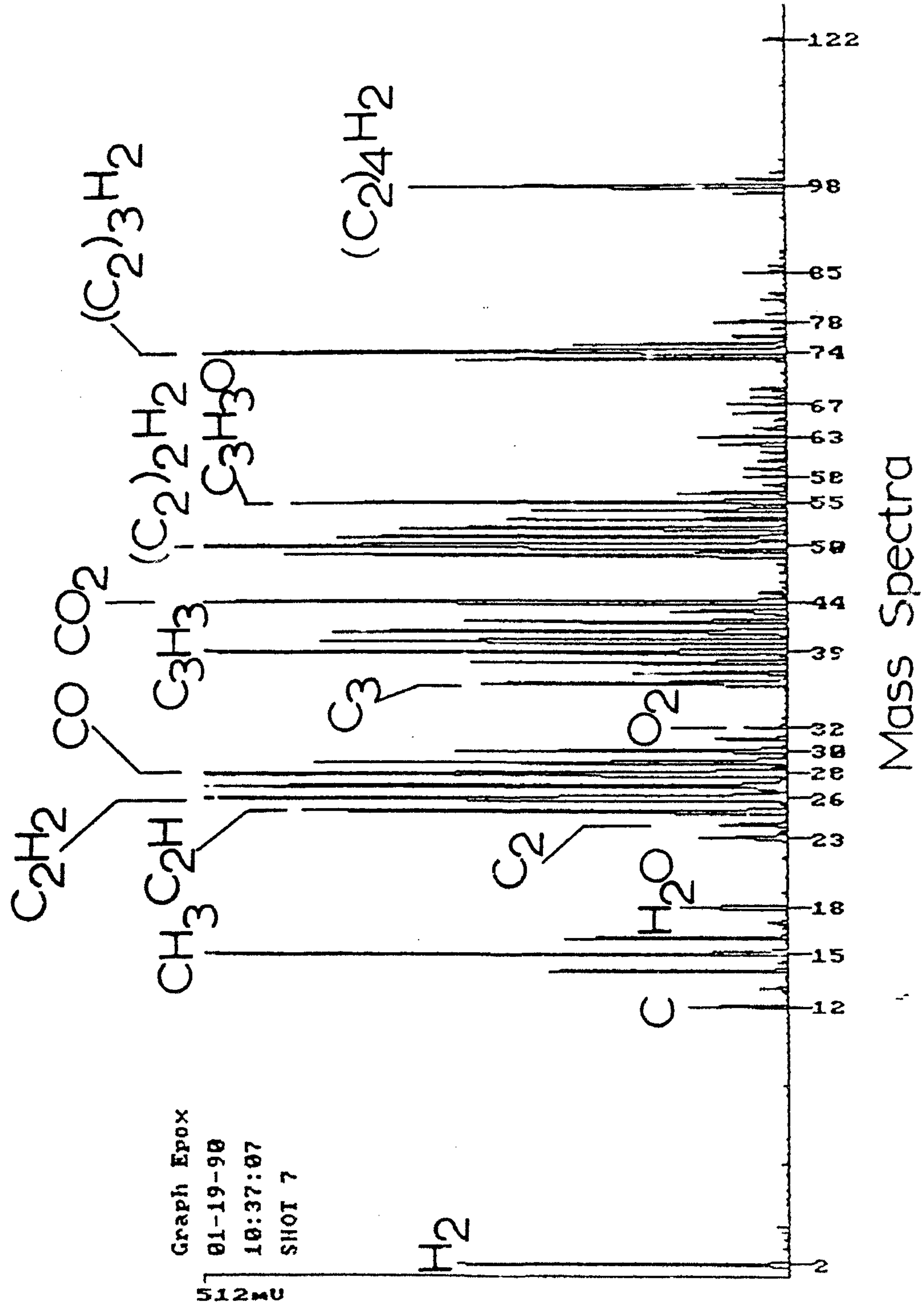

Figure 3. The TOFMS spectrum for ablation plume characterization showing typical mass fraction (mass-to-atom ratio)/fragment analysis after 7 pulses.

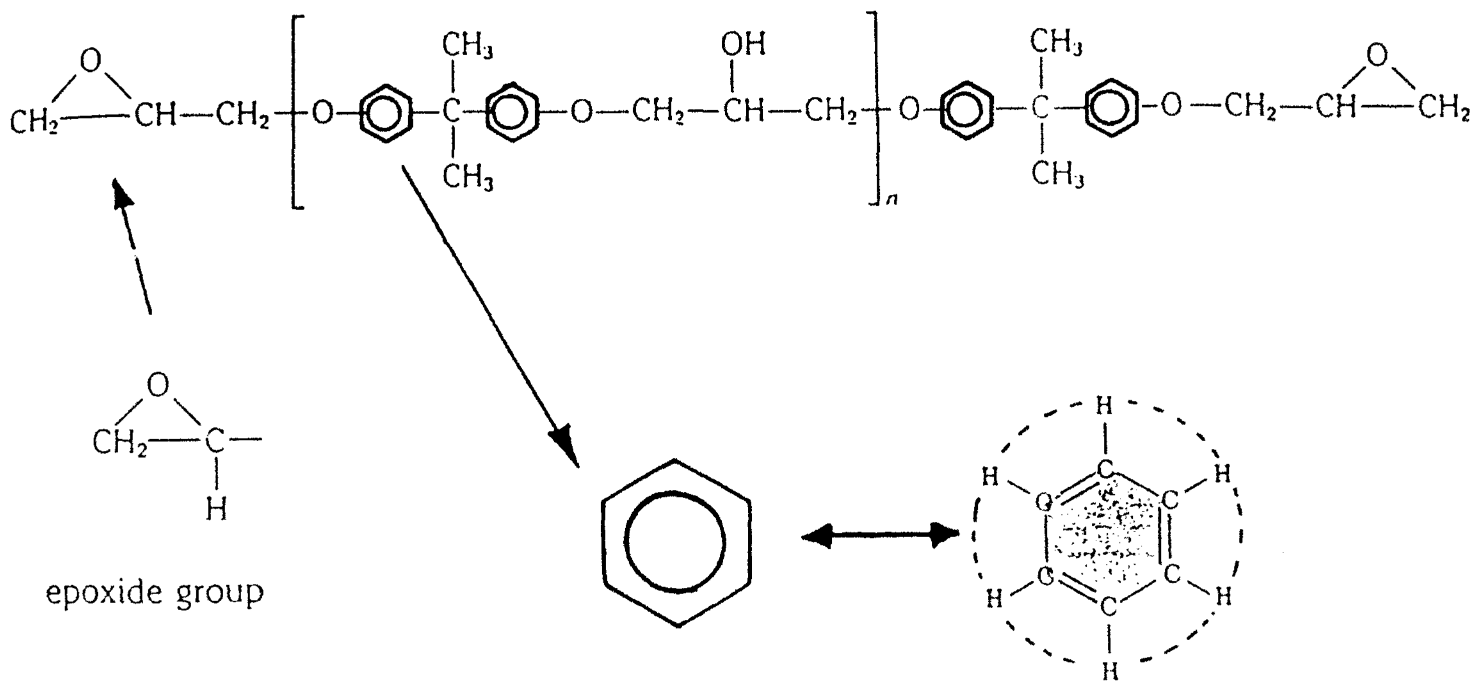

Figure 4. Simple epoxy chemical structure showing epoxide group and benzene-ring-containing polymer structure groups. The circles and dotted circles represent hydrogen groupings.

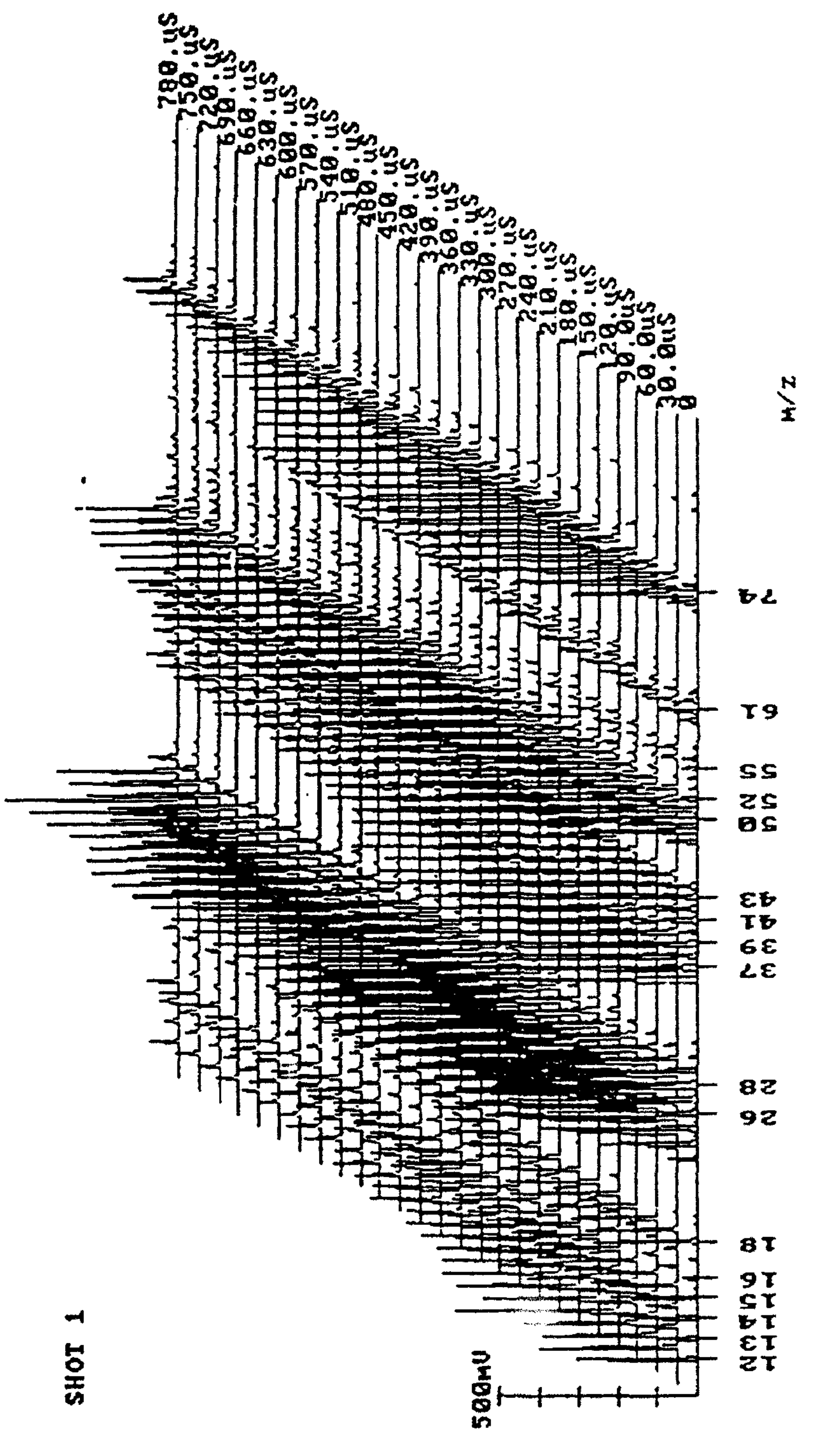

(a) Single ablation (pyrolysis) pulse.

Figure 5. Time-resolved TOFMS spectra comparing a single ablation (pyrolysis) pulse and four pulses.

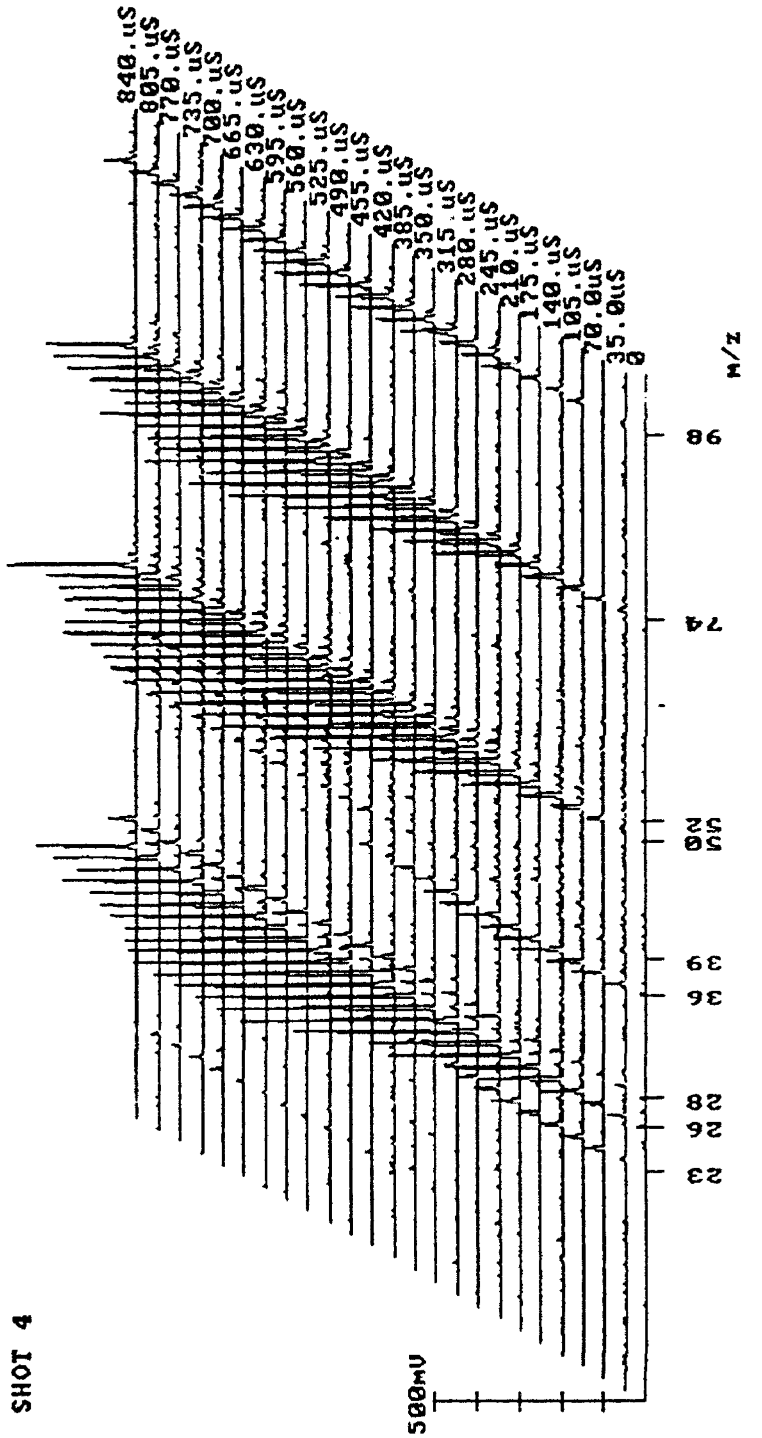

(b) Four pulses.

Figure 5. Concluded.

the corresponding heats of formation of the different species ($H_{epoxide}$ = 260 kCal/mol; $H_{acetylene}$ = 333 kCal/mol; H_{C3} = 480 kCal/mol). In fact, the carbons were generated before the acetylenes. The C_3 was assumed to be a product of laser decomposition of the epoxide component deposited on the sample surface.

The surface vaporization temperature of the C_3 component, for example, can be calculated from a simple gas dynamic model for a hypersonic free jet expanding adiabatically as illustrated previously by K. A. Lincoln (Refs. 8 and 9) to be about 4700 K. The C_3 also apparently emanates as free radicals but with less affinity for the surface than the epoxides. The moderate life spans of carbon seen in the TOFMS spectra may be attributed to the fact that C_3 is a condensable, which is represented by the symmetry of the C_3 spectrum in the time versus intensity data illustrated in Figure 5. On examining the carbon grid surfaces in the TEM, a variety and distribution of deposited "particles" were observed. These particulates assumed a variety of morphologies ranging from apparent "spheres", to faceted polyhedra, and plate-like morphologies to sheetlike fragments. Some individual particles aggregated, and some of these aggregates contained contaminating particulates. Many aggregates contained growth features such as rosettes and spiral structures typical of high quality (pure) graphites (Ref. 10). These morphological features are illustrated in the examples reproduced in Figures 6 through 8.

The crystallographic features unique to graphite and implicit to some extent in Figures 6 through 8 are illustrated in more detail in the examples shown in Figures 9 and 10. These examples, together with those shown in Figures 6 through 8, suggest a wide range of graphite ablation fragments either as a direct consequence of graphite fiber damage or "condensation" of carbon fragments in the plume composition from the epoxy matrix. The TEM observations in Figures 6 through 10, taken together with the plume spectra shown in Figures 3 and 5, suggest a complex set of ablation-related phenomena which include both the graphite fibers and the deposition of graphite fragments which result from laser-induced decomposition (pyrolysis) of the epoxy matrix. Indeed, it is well known that destructive shock wave reactions/interactions can break molecular bonds leading to either isomerization or polymerization (Refs. 11 and 12). In the crystallization of low molecular weight fractions from the melt at high temperatures, it is possible to obtain extended chain crystals in which the distribution of crystal thickness approximates the

(a) Secondary electron (SEM-mode) particle image.

(b) STEM-mode image of cluster.

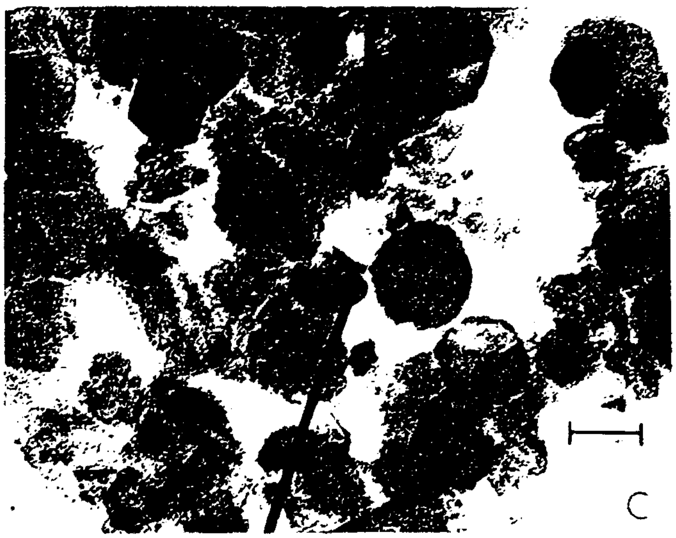

(c) Hexagonally-faceted graphite particles observed in CTEM mode. Magnification markers are 0.05 μm.

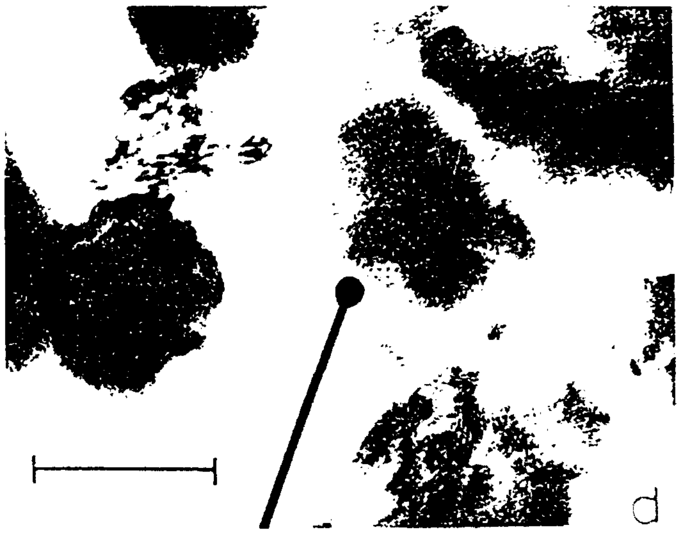

(d) Variations of CTEM particle images. Magnification markers are 0.05 μm.

Figure 6. Examples of graphite deposition residue (particulates) collected on TEM carbon-coated grids.

(a) Rosette particles.

Figure 7. Rosette and thin flake (plate-like) graphite particles deposited on carbon-coated grids in ablation blow-off plume as observed in the TEM (bright-field images).

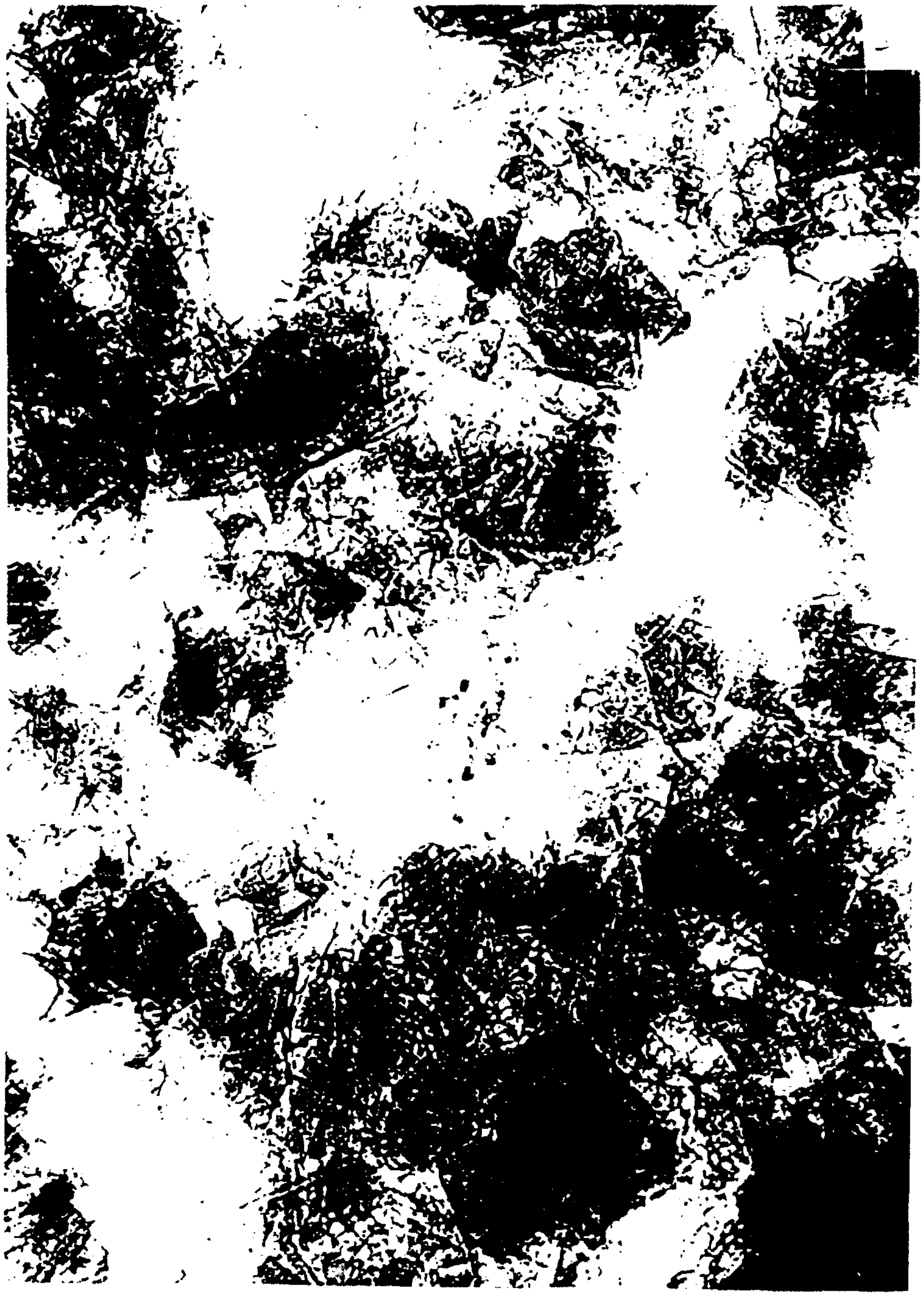

(b) Thin flake (plate-like) graphite particles.

Figure 7. Concluded

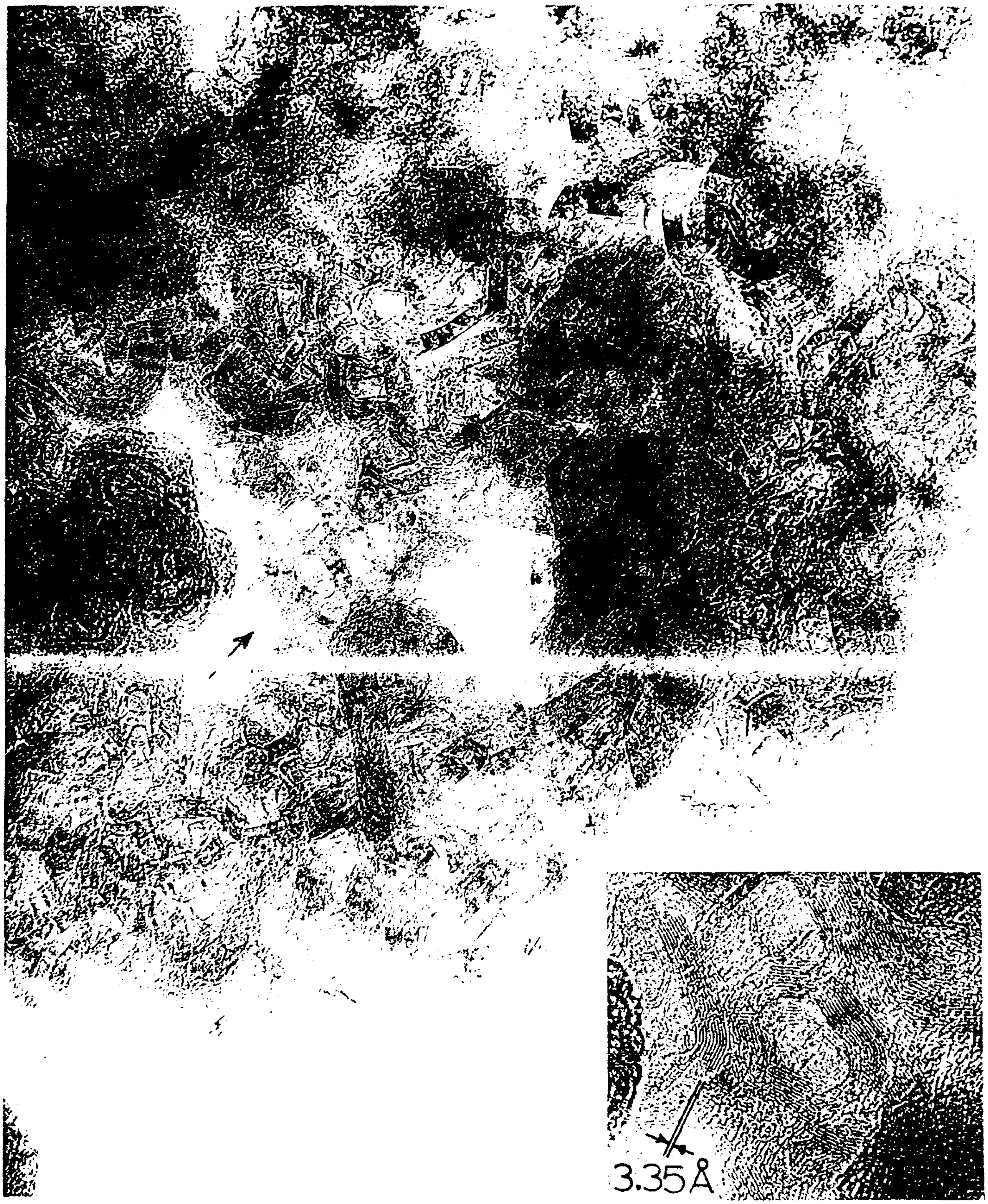

Figure 8. Standard, high-purity graphite lattice-image standard showing growth features and polycrystalline structures. Insert shows lattice image details for micro-rosette growth.

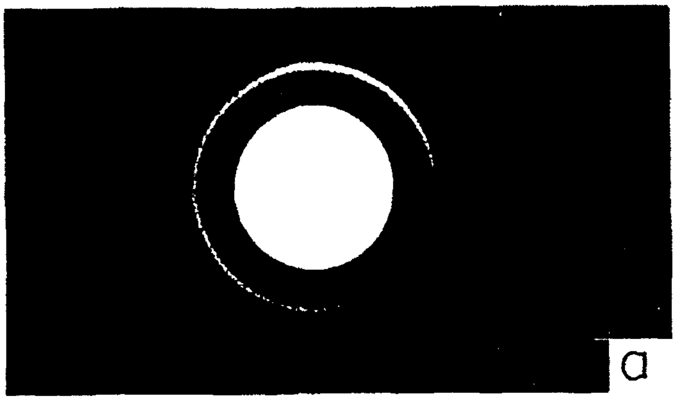

(a) "Amorphous" reference diffraction pattern for the carbon support film composing the TEM grid collector.

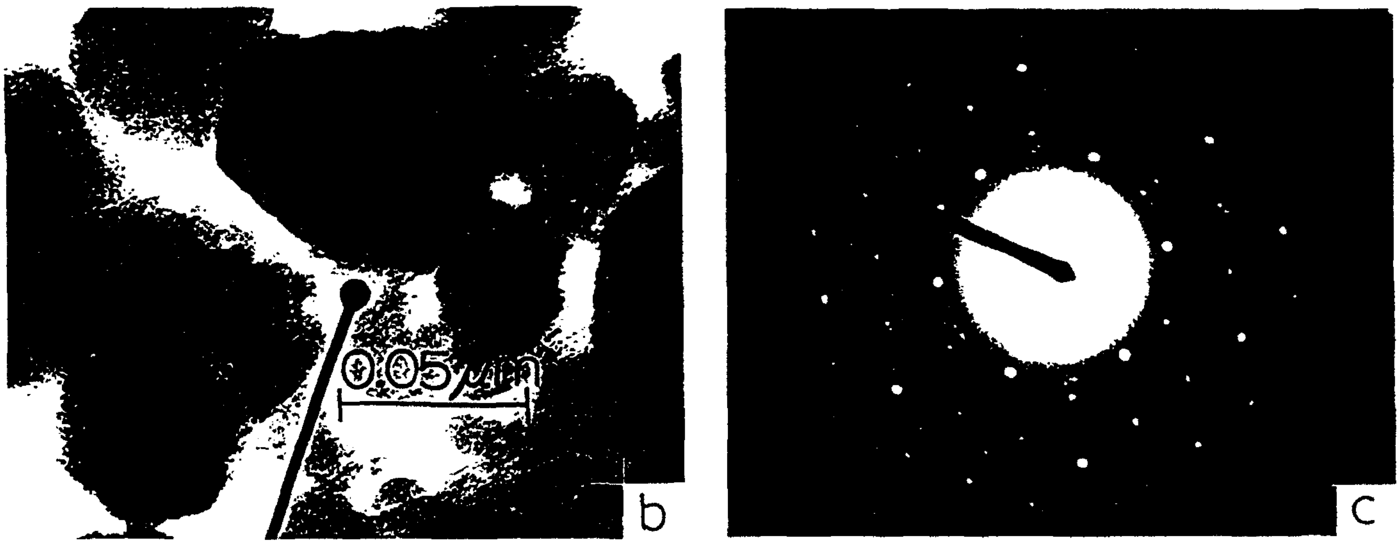

(b) The TEM (bright-field) image showing facets characteristic of hexagonal graphite crystals oriented parallel to basal (0001) plane confirmed by (c).

(c) The selected-area electron diffraction spot pattern.

Figure 9. Crystallinity and crystal morphology in deposited (hexagonal) graphite.

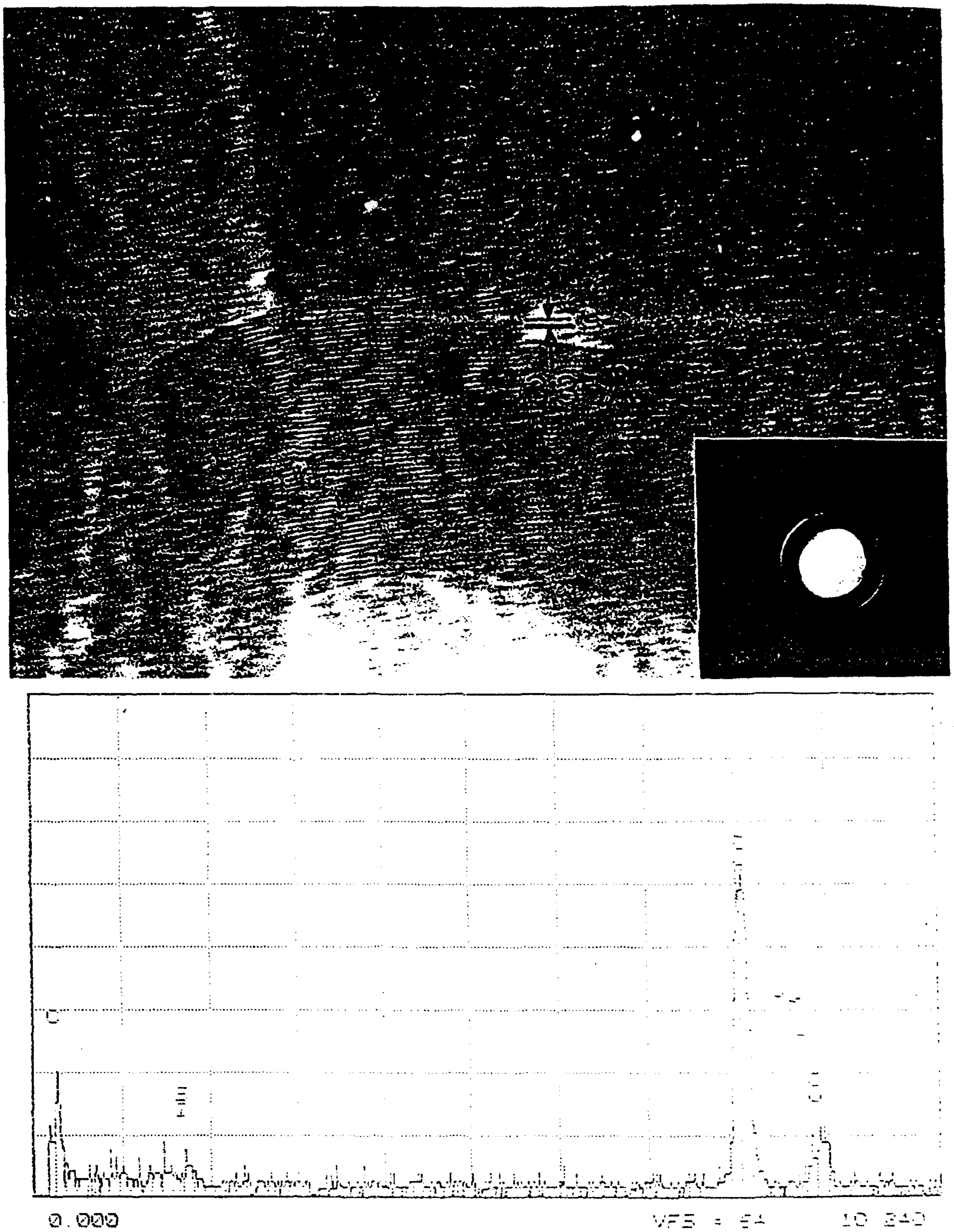

Figure 10. Polycrystalline and textured (oriented) graphite platelets showing lattice fringes for (0002) basal plane spacing. The selected-area electron diffraction pattern insert shows the polycrystalline, fine crystal texture implicit in the TEM image while the energy-dispersive x-ray spectrum shows the elemental carbon peak characteristic of the graphite structure. The copper peaks represent the copper support grid and serve as a calibration standard.

distribution of chain lengths (Ref. 13). A polymer molecule in the vicinity of a surface has its entropy decreased and its free energy increased in comparison to a molecule not so impeded (Ref. 14). Consequently, the combination of localized high temperature, shock spallation and shock heating as well as shock energy localization can cause fragmentation and re-combination (condensation) as illustrated schematically in Figure 11. This process produces a wide range of crystalline and polycrystalline (hexagonal) graphite particulates and aggregates as illustrated in Figures 6 through 10, and consistent with the spectra shown as typical in Figure 3. While other carbon variants were investigated (such as the higher forms of C_n: C_{40}, C_{60}, C_{70}, etc.) the analyses only identified various forms (crystallinity and polycrystallinity in a variety of morphologies ranging from spheroids to platelets) of hexagonal graphite.

4.0 CONCLUSIONS

Scanning electron microscopy (SEM) was used to examine the macroscopic features of laser ablation damage to a G/E composite along with TOFMS to examine the pulsed plume emission during ablation, and TEM to observe debris and deposition fragments resulting from the ablation process. The total picture which emerges from these observations involves laser shock damage fragments along with pyrolysis components, all of which are finally deposited some distance (~5 cm) from the ablation zone. These deposited particulates include a wide range of hexagonal graphite morphologies and crystal structures which include direct fragmentation (or spallation) from the graphite fibers in the composite along with shock and pyrolysis-induced graphites which originate from the molecular fragmentation and carbon condensation from the epoxy matrix.

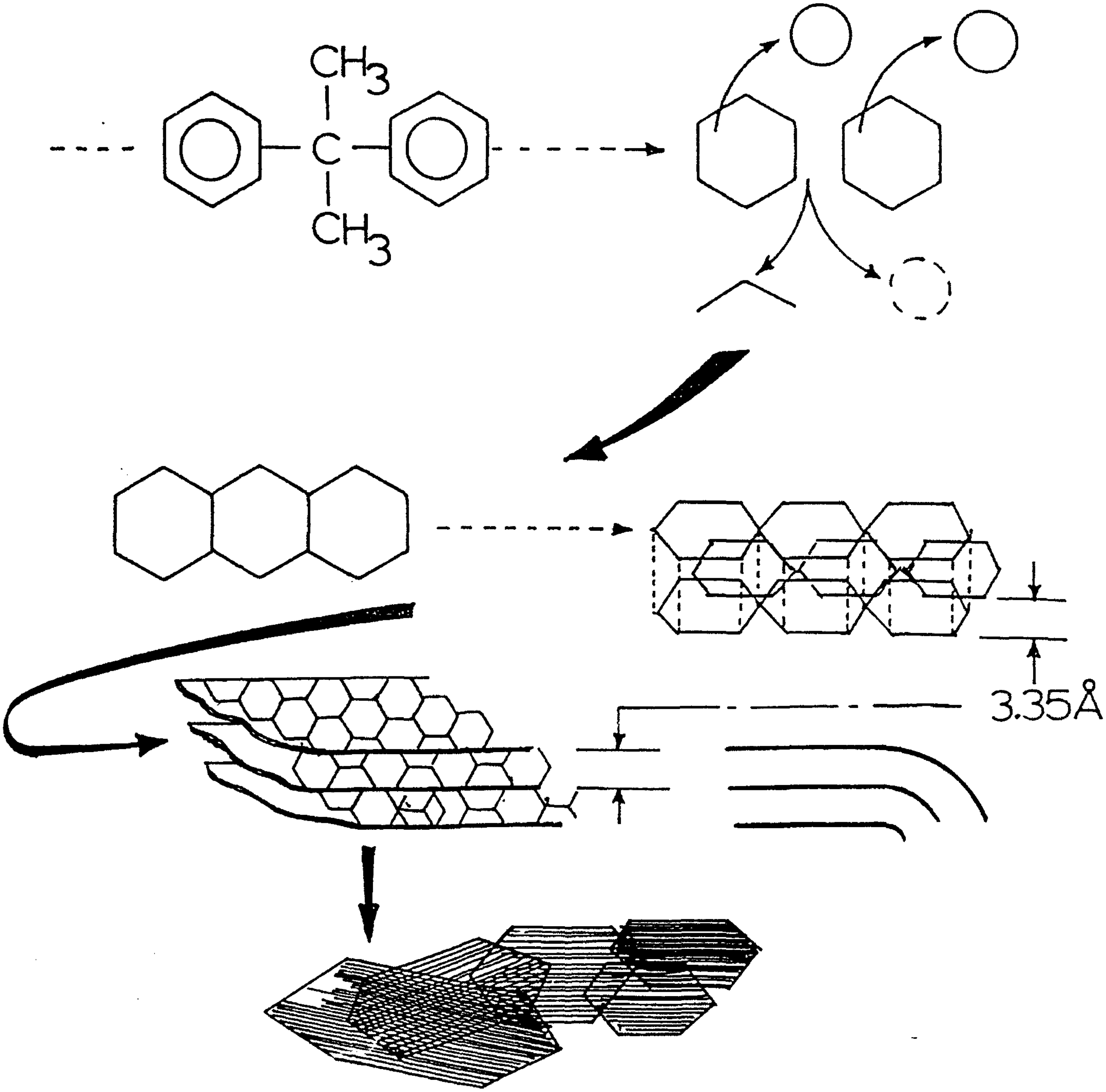

Figure 11. Schematic representation of a simple molecular fragmentation model to produce graphite particulates in the ablation blow-off plume for laser-irradiated G/E composite. In this simple model, laser-shock-induced hydrogen fragmentation leaves C_3 and C_6 benzene groups which recombine to form various shapes and periods of crystalline and polycrystalline hexagonal graphites.

While it is impossible to differentiate between the shock-induced and pyrolysis-induced deposition of graphite particulates on surfaces away from the ablation zone, it might be assumed that similar phenomena would occur in hypervelocity particle impacts with G/E composite materials in space. The important aspects of these ablation and hypervelocity impact phenomena are concerned with the potential for altering, compromising, or degrading sensor, optical, or control surfaces as a consequence of graphite deposition from a vapor plume. This scenario may be especially important in alteration of the electrical conductivity of neighboring components, a consequence of graphite deposition from impacted polymeric materials in general if elemental carbon is redeposited as graphite. In this regard, there was no evidence in this work for other, higher carbon complexes (fullerenes) such as C_{40}, C_{60}, C_{70}, etc., or of crystalline diamond.

REFERENCES

1. Damage in Laser Glass, A.J. Glass and A.H. Guenther, Eds., ASTM Special Technical Publication 469, ASTM, Philadelphia, PA, 1969.

2. Laser Induced Damage in Optical Materials: 1976, A.J. Glass and A.H. Guenther, Eds., NBS Special Publication 462 (also printed as ASTM Special Technical Publication 622), U.S. Govt. Printing Office, 1976.

3. Rubin, I., Chou, M.S., Repetitively Pulsed Laser Effects Phemenology Program, AFWL-TR-88-112, Air Force Weapons Laboratory, Kirtland AFB, NM, 1987.

4. Clauer, A.H., Holbrook, J.H. and Fairand, B.P., "Effects of Laser Induced Shock Waves on Metals," Shock Waves and High-Strain-Rate Phenomena in Metals, Chap. 38, p. 675, M.A. Meyers and L.E. Murr, Eds., Plenum Press, New York, NY, 1981.

5. Batsanov, S.S., Physical Chemistry of Shock-induced Compression: A New Scientific Trend Comes into Being, Izvestia, Siberian Academy of Sciences, Chemical Series, 676, November 6, 1967.

6. Batsanov, S.S., "High Pressure Inorganic Chemistry, Russian Chemical Reviews, 55(4), 297, pp 579-607, 1986.

7. Lincoln, K.A., Bechtel, R.D., A Fast Data Acquisition System for the Study of Transient Events by High Repetition Rate Time-of-Flight Mass Spectrometer, NASA Technical Memorandum 88374, National Aeronautics and Space Administration, Washington, DC, 1986.

8. Lincoln, K.A., "Experimental Determination of Vapor Species from Laser-Ablated Carbon Phenolic Composites," AIAA Journal, 21:2, 1983.

9. Lincoln, K.A., Covington, A.M., "Dynamic Sampling of Laser-Induced Vapor Plumes by Mass Spectrometry," International Journal of Mass Spectrometry and Ionic Processes, 16, pp 191-208, 1975.

10. Ijima, S.,"The 60-Carbon Cluster Has Been Revealed!," J. Phys. Chem., 91: 3466, 1987.

11. Hermann, W., "Constitutive Equation for The Dynamic Compaction of Ductile Porous Materials," J. Appl. Phys., 40: 2490, 1969.

REFERENCES (Concluded)

12. Sekine, T., "Shock Recovery Experiment of Carbon," Shock-Wave and High-Strain Rate Phenomena in Materials, Chap. 28, p. 311, M.A. Meyers, L. E. Murr and K. P. Staudhammer (Eds.), Marcel Dekker, Inc., New York, NY, 1992.

13. Anderson, F.R.,"Morphology of Isothermally Bulk-Crystallized Linear Polyethyleney," J. App. Phys., 35: 64, 1964.

14. Lindenmeyer, P.H., Frontiers in Materials Science, Chap. 6, p. 219, L.E. Murr and C. Stein (Eds.), Marcel Dekker, Inc., New York, NY, 1976.

DISTRIBUTION

AFSAA/SAI, Washington, DC
AUL/LSE, Maxwell AFB, AL
DTIC/OCC, Alexandria, VA
PL/SUL/HO, Kirtland AFB, NM
Official Record Cy
  PL/VTSI, Kirtland AFB, NM